JACS
JOURNAL OF THE AMERICAN CHEMICAL SOCIETY
Communication
pubs.acs.org/JACS

Elusive O═P≡N, a Rare Example of Phosphorus $\sigma^2\lambda^5$-Coordination

Xiaoqing Zeng, Helmut Beckers,* and Helge Willner

FB C-Mathematik und Naturwissenschaften-Fachgruppe Chemie, Bergische Universität Wuppertal, D-42097 Wuppertal, Germany

Supporting Information

ABSTRACT: Two linear isomers, OPN and ONP, were formed in an Ar matrix at 16 K by ArF laser (λ = 193 nm) photolysis of phosphoryl triazide, $OP(N_3)_3$, and comprehensively characterized by their mid- and far-IR spectra as well as $^{14/15}N$ isotopic data. Two intermediates, $(N_3)_2P(O)N$ and $N_3P(O)N_4$, have been isolated in an Ar matrix and spectroscopically characterized. Photolysis of these intermediates using near-UV/vis light (λ > 320 nm) was shown to yield exclusively ONP, which under ArF laser irradiation selectively photo-isomerized to OPN. The photochemical and molecular properties of OPN and ONP are discussed on the basis of experimental and *ab initio* calculated results.

Multiple-bond phosphorus compounds are known to be useful building blocks in organophosphorus chemistry.[1] Those bearing triply bonded phosphorus are mostly restricted to phosphorus at low oxidation states. Examples are phosphaalkynes RC≡P,[2] the parent phosphaethyne HC≡P, which is a highly reactive colorless gas that polymerizes rapidly above −124 °C,[3] and phosphorus nitride P≡N, which can be considered as the simplest azaphosphyne (phosphazyne). Diatomic P≡N has been attracted much interest[4] since its detection in interstellar clouds as well as in the atmospheres of Jupiter and Saturn.[5] Triply bonded $\sigma^2\lambda^5$-phosphorus is very scarce and, to our knowledge, restricted to diphosphyne derivatives P≡P═O[6] and P≡P═S.[7] These were detected in microwave-discharged gas mixtures of $Ar/P_4/O_2$ and $Ar/P_4/S_8$, respectively.

Of particular interest is the linear ONP molecule, first identified when solid $Ar/PN/^{16}O_3/^{18}O_3$ mixtures were subjected to near-UV photolysis (λ > 310 nm),[8] and later observed in $NO/P_4/O_2$/noble-gas mixtures by gas-phase IR laser absorption spectroscopy,[9] as well as in a dc glow discharge of NO/H_2 over red phosphorus by microwave spectroscopy.[10] The isomeric OPN molecule has never been detected, and because only the phosphorus(III) isomer was detected in previous experiments, it has been concluded that phosphorus(V) avoids two-fold coordination.[8] This statement was further supported by several theoretical studies, which predicted a higher stability of ONP compared to OPN.[8,11,12] The widely accepted argument for the predicted lower stability of OPN was the proposed reluctance of phosphorus to form strong multiple bonds.[11,12] This destabilizing effect was assumed to overcompensate any electrostatic stabilization arising from the most electropositive atom located in the molecular center.

However, this common belief has not been proved rigorously, and recently a high-level CCSD(T)/aug-cc-pV(T+d)Z study claimed a reversed stability order, with OPN 7.1 kJ mol^{-1} *lower* in energy than ONP at 0 K.[13] The new results raise the question, why has only the less stable isomer ONP been observed experimentally? In the former gas-phase studies, in which NO and P atoms might be present in the reactive mixtures, P atoms can add to the terminal N of NO to form ONP, but they are unlikely to insert into the strong NO bond to form OPN.[13] On the other side, configuration interaction (CI) calculations[11] revealed a significant barrier of 296 kJ mol^{-1} for the rearrangement of ONP through a cyclic isomer to OPN, which explains the difficulty in obtaining OPN by thermal isomerization of ONP in the gas phase. Such arguments, however, cannot account for the absence of the more stable OPN in previous matrix-isolation experiments, in which the reaction of PN with photo-generated O atoms was studied.[8]

Furthermore, the phosphorus(V) isomer OPN is likely detectable in circumstellar and dense interstellar clouds where phosphorus- and nitrogen-containing molecules have been discovered.[14] The recent direct observation of PN in the supergiant star VY CMa implies the possible existence of OPN isomers in the presence of oxygen.[15] Thus, there were strong reasons to re-investigate the ONP/OPN system, to provide more rigorous proof for the existence of the elusive OPN isomer. In our approach to this missing isomer, we used the matrix-isolation technique, starting from the triazide precursor $OP(N_3)_3$, recently isolated in neat form.[16] This study continues our previous investigation on the related 2,2-difluoro-aza-λ^5-phosphyne (NPF_2),[17] prepared by photo-decomposition of the monoazide F_2PN_3, as well as the synthesis of the elusive cyclic diazirinone (OCN_2, C_{2v}) from carbonyl diazide ($OC(N_3)_2$).[18]

Covalent azides usually exhibit strong UV absorptions around 200 nm. Thus, a mixture of $OP(N_3)_3$/Ar (~1:1000) was deposited as an Ar matrix at 16 K and subjected to ArF excimer laser irradiation (λ = 193 nm). According to the IR spectrum recorded from the deposit (Supporting Information (SI) Figure S1), >50% of the triazide decomposed, and several weak bands appeared simultaneously. The new bands can be divided into four sets, assigned to four different photo-products according to their specific photo-behavior and characteristic IR spectra. First the photo-products were subjected to visible light irradiation (λ > 420 nm), and the resulting IR difference spectrum is shown in Figure 1.

The precursor bands are not affected by visible light; however, one set of the product bands disappeared completely, while the bands of the other proto-products increased simultaneously. From the difference spectrum (Figure 1), the

Received: September 29, 2011
Published: November 23, 2011

ACS Publications © 2011 American Chemical Society

dx.doi.org/10.1021/ja2091867 | J. Am. Chem.Soc. 2011, 133, 20696–20699

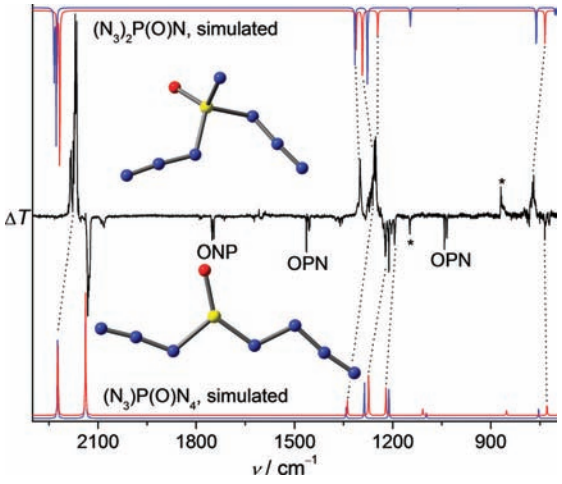

Figure 1. Calculated IR spectra (DFT B3LYP/6-311+G(3df), scaled by a factor of 0.9679) of $(N_3)_2P(O)N$ (top) in the triplet (red line) and singlet (blue line) states, and of *cis* (red line) and *trans* (blue line) $N_3P(O)N_4$ (bottom). The middle trace displays the IR spectral changes upon visible light irradiation (λ > 420 nm, 20 min) after laser photolysis (λ = 193 nm) of $OP(N_3)_3$, showing depletion of the initially formed $(N_3)_2P(O)N$ (upward) and formation of the secondary products (downward). The carriers of the two bands marked by asterisks are unknown.

IR spectrum of the photo-labile product (pointing upward) is picked out. Its main bands are located at 2169.8, 1299.5, 1255.4, and 772.4 cm^{-1}, tentatively attributed to vibrational stretching modes of an azide group [$\nu_{as}(N_3)$, $\nu_s(N_3)$], ν(PO), and ν(PN), respectively. These band positions are close to the corresponding fundamentals of the triazide precursor [2172.4 $\nu_{as}(N_3)$, 1311.5 ν(PO), 1258.7 $\nu_s(N_3)$, and 781.2 cm^{-1} $\nu_{as}(PN_3)$].[16] Experiments using ^{15}N-trisubstituted $OP(N_3)_3$ revealed an $^{14/15}N$ isotopic shift for each band (SI Figure S2), although determination of individual $^{14/15}N$ shifts is hampered due to interference from six isotopomers of the triazide precursor.[19] The spectrum of the photo-labile species was assigned to the phosphoryl nitrene $(N_3)_2P(O)N$, initially formed from $OP(N_3)_3$ by eliminating one N_2 molecule. This assignment is supported by (i) the similarity of its IR spectrum to that of the precursor; (ii) its photo-destruction products (Figure 1); (iii) calculated IR spectra at the DFT B3LYP/6-311+G(3df) level for both singlet and triplet nitrene (SI Table S1), which show good agreement with experimental spectra, especially for the triplet species (Figure 1); (iv) DFT calculations of the relative energies of the two lowest electronic states, which revealed a triplet ground state of $(N_3)_2P(O)N$ with a triplet−singlet energy gap of 84 kJ mol^{-1}; and (v) the presence of visible electronic transitions. Triplet oxo−nitrenes were shown to exhibit up to two visible transitions,[20] and the vertical transition energies for the visible bands of $(N_3)_2P(O)N$ are predicted by time-dependent (TD) DFT B3LYP/6-311+G(3df) calculation at 586.95 (f = 0.0018) and 552.46 nm (f = 0.0007).

Unlike simple nitrenes, which usually feature low-lying open-shell singlet and triplet electronic states, oxo−nitrenes show nearby triplet and closed-shell singlet electronic states, since the singlet state is stabilized by an intramolecular oxygen−nitrene lone-pair interaction.[20] This interaction lowers the position of the corresponding P═O and P—N fundamental frequencies. Thus, the IR spectra of the two lowest electronic states of $(N_3)_2P(O)N$ can be distinguished by the position of the fairly strong P═O fundamental, predicted at 1287 and 1184 cm^{-1} for the triplet and singlet species, respectively (calculated structures and IR frequencies are given in SI Figure S3 and Table S1, respectively). For the triplet nitrene, the P═O fundamental (1255.4 cm^{-1}) appeared close to $\nu_s(N_3)$, while no feature can be assigned to the P═O mode of the singlet species (Figure 1).

Characteristic IR features of the products formed by photo-destruction of $(N_3)_2P(O)N$ are shown in Figure 1. These photo-products were further distinguished by their behaviors upon near-UV/vis irradiation (λ > 320 nm). Complete IR spectra obtained from the natural and ^{15}N-trisubstituted $OP(N_3)_3$ are displayed in SI Figures S2, S4, S5, and S6.

A representative photo-reaction by visible light irradiation of the previously investigated azido oxo−nitrenes is migration of the N_3 substituent to the electron-deficient nitrene center.[21] For $(N_3)_2P(O)N$, this Curtius-type rearrangement furnished $N_3P(O)N_4$, in which N_3 and N_4 substituents are linked to phosphorus. DFT calculations for this novel species revealed two strong and characteristic IR bands at 2222/2224 and 2138/2138 cm^{-1} (*cis*/*trans* conformers) corresponding to the very different $\nu_{as}(N_3)$ modes of the N_3 and N_4 moieties, respectively. *Cis*/*trans* refers to the orientation of the P═O and N^{α}–N^{β} bonds with respect to the P═N^{α} bond (SI Figure S3).

Indeed, two strong bands at 2172.4 and 2127.9 cm^{-1} increased upon photo-destruction of the nitrene $(N_3)_2P(O)N$ by visible light irradiation (Figure 1, middle trace) and diminished completely upon near-UV/vis irradiation (λ > 320 nm). Figure 1 compares spectra calculated for *cis* and *trans* $N_3P(O)N_4$ (SI Table S1) to the experimental spectrum. The *cis* conformer was calculated to be slightly lower in energy (7 kJ mol^{-1}, B3LYP/6-311+G(3df)) than the *trans*. The 2172.4 cm^{-1} absorption of $N_3P(O)N_4$ overlapped with the strong azide band of the nitrene in Figure 1. However, the nitrene is rapidly destroyed by visible light, and this interference does not appear in the difference spectra obtained after subsequent near-UV/vis experiments (SI Figures S5 and S6). According to TD DFT calculations, the near-UV transition of $N_3P(O)N_4$ can be attributed to the π(P═N^{α}) bond linked to the N_4 substituent. This orbital mainly contributes to the highest occupied molecular orbital (HOMO, A″) and is part of a conjugated system involving the two azido substituents. The calculations suggest two rather weak transitions to virtual orbitals of A′ symmetry at 375 (f = 0.0006) and 333 nm (f = 0.0009). Further, a rather low barrier of 38 kJ mol^{-1} for N_3 migration in excited singlet nitrene was predicted by DFT calculations. Thus, the agreement between calculated and experimental results is conclusive, and the assignment of this second $P(O)N_7$ isomer is quite definite.

Two photo-products of $OP(N_3)_3$ remained to be assigned and were easily identified as the ONP/OPN isomers. The known bands of ONP in solid Ar[8] are readily figured out from the spectrum. Apart from some un-decomposed precursor, ONP is the sole product that eventually formed after near-UV/vis irradiation (λ > 320 nm) of the deposit. Thus, both OPN and $N_3P(O)N_4$, which survived the preceding visible light irradiation, are selectively transformed by near-UV/vis light into ONP and ONP + $3N_2$, respectively.

Two sharp doublets at 1751.9/1747.7 and 866.1/862.1 cm^{-1} are assigned to ν(NO) and ν(PN) of ONP, respectively. The positions of these bands match well to those reported in the former Ar matrix-isolation study (1754.7 and 865.2 cm^{-1}).[8] These doublets are probably due to matrix site splittings in the

dx.doi.org/10.1021/ja2091867 | J. Am. Chem.Soc. 2011, 133, 20696–20699

presence of nitrogen molecules, formed by decomposition of the triazide precursor. The hitherto missing bending mode of ONP is now found as a doublet at 461.4/458.2 cm^{-1} (SI Figure S4).

In addition to the three IR fundamentals, the combination band $\nu_2 + 2\nu_3$ and the overtone band $2\nu_2$ of ONP were also observed at 1789.8/1785.4 and 1721.7/1714.1 cm^{-1}, respectively (Figure 2). The overtone $2\nu_2$ receives its intensity from

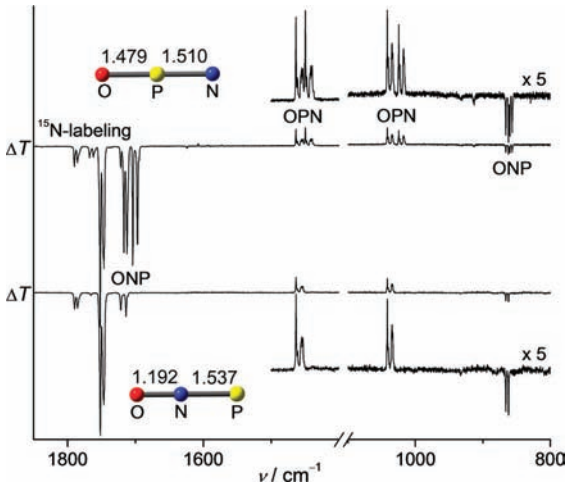

Figure 2. IR spectral changes in the region of 1850−800 cm^{-1} obtained upon near-UV/vis light irradiation (λ > 320 nm, 20 min) of an Ar matrix containing the photolysis products of natural (lower trace) and ^{15}N-labeled $OP(N_3)_3$ (upper trace), which were subjected to preceding ArF laser (λ = 193 nm) and visible light (λ > 420 nm) photolysis. The IR bands are assigned to either OPN (upward) or ONP (downward), and their CCSD(T)/cc-pVTZ molecular structures and bond lengths (Å) are shown. The full spectra recorded in the region of 2220−700 cm^{-1} are given in SI Figures S6 (natural) and S7 (^{15}N-labeled).

Fermi resonance from the N═O stretching mode (ν_1), manifested particularly by the strong increase in intensity for $2\nu_2$ of ^{15}N-labeled O^{15}NP (Figure 2), as well as by a strong deviation of the experimental $^{14/15}$N isotopic shifts of the Fermi couple from the calculated harmonic ones (Table 1, top).

Table 1. Experimental (Ar Matrix) and Calculated (Harmonic) IR Frequencies, $^{14/15}$N Isotopic Shifts ($\Delta\nu$, cm^{-1}, CCSD(T)/cc-pVTZ), and Intensities (in Parentheses, km mol^{-1}, MP2/cc-pVTZ//CCSD(T)/cc-pVTZ) of ONP and OPN

mode	ν_{exptl}	ν_{calcd}	$\Delta\nu_{exptl}$	$\Delta\nu_{calcd}$
		ONP		
$\nu_2 + 2\nu_3$	1789.8/1785.4		22.3	25.8
ν_1	1751.9/1747.7	1815 (284)	35.0	41.3
$2\nu_2$	1721.7/1714.1		17.8	5.6
ν_2	866.1/862.1	876 (2)	5.9	2.8
ν_3	461.4/458.2	464 (3)	11.4	11.5
		OPN		
ν_1	1463.4/1454.8	1459 (8)	13.9	15.7
ν_2	1041.7/1034.8	1030 (36)	17.0	16.7
ν_3	234.1/232.2	225 (17)	1.9	2.2

Two rather weak doublets at 1463.4/1454.8 and 1041.7/1034.8 cm^{-1} in the mid-IR region (Figure 2) and the one at 234.1/232.2 cm^{-1} in the far-IR spectrum (SI Figure S4) are convincingly assigned to the three fundamentals of the novel OPN molecule (Table 1, bottom). This assignment is further proved by the conformity of the experimental and calculated $^{14/15}$N isotopic shifts. The large $^{14/15}$N isotopic shifts for both stretching modes in OPN indicate strong coupling between them; they are described as in-phase and out-of-phase OPN stretches. In contrast, the quite small $^{14/15}$N shift for the bending mode (ν_3) is more consistent with a wagging mode, where almost exclusively the oxygen atom is involved.

With the formation of ONP and OPN convincingly proved, we explored their reversible interconversion in further photolysis experiments. As already mentioned, near-UV/vis light (λ > 320 nm) selectively transforms OPN into ONP. Thus, if any OPN were formed in the previously studied reaction of PN + O atoms,[8] it would have been rapidly photoisomerized by the λ > 310 nm radiation used to generate O atoms from O_3. TD DFT calculation mainly attributes the predicted electronic OPN transition at 366 nm (f = 0.0156) to a HOMO−LUMO excitation: one electron is excited from the degenerate nonbonding (allylic) π(O═P═N) orbital to the antibonding σ*-combination of phosphorus 3s with the σ(p) orbitals of the nitrido and oxo substituents (LUMO).[22]

$$\mathrm{OPN} \underset{\lambda=193\ \mathrm{nm}}{\overset{\lambda>320\ \mathrm{nm}}{\rightleftharpoons}} \mathrm{ONP}$$

On the other hand, ArF laser irradiation (λ = 193 nm) led to quantitative conversion of ONP to OPN (SI, Figure S5). This is accounted for by TD DFT calculations, which predict the lowest-energy electronic transition of ONP at 191 nm (f = 0.0423). Hence, photolysis enabled reversible interconversion between ONP and OPN. In addition, prolonged ArF laser irradiation of the triazide will eventually accumulate OPN, since both the $P(O)N_7$ intermediates and ONP are depleted by ArF laser light.

The structures of OPN and ONP were fully optimized using both DFT (B3LYP/6-311+G(3df)) and *ab initio* (CCSD(T)/cc-pVTZ) methods. The results are consistent with previous high-level *ab initio* studies.[13] At the CCSD(T)/cc-pVTZ level of theory, the P−N bond length in OPN (1.510 Å) is shorter than that of ONP (1.537 Å); both are well within the sum of the covalent radii for P and N for triple (1.48 Å) and double bonds (1.62 Å).[23] The O−P bond length in OPN (1.479 Å) is also significantly shorter than the sum of the corresponding atomic double-bond covalent radii (1.59 Å), while the O−N bond length in ONP (1.192 Å) is longer (1.17 Å).[23] Natural population analysis of OPN reveals a significant positive partial charge on the central P (+2.06 e) and almost equivalent negative charges on O (−1.02 e) and N (−1.04 e), while the O atom in ONP is significantly more negatively charged (−0.42 e) than the N atom (−0.16 e). Appropriate Lewis resonance structures of the two isomers are depicted below. Oxygen lone-pair delocalization into the π*(PN) orbitals of OPN can account for strengthening of the O═P bond at the expense of the P≡N triple bond.

To conclude the photochemistry of $OP(N_3)_3$ in Ar matrices at 16 K (Scheme 1), its initial photo-decomposition yields two intermediates, $(N_3)_2P(O)N$ and $N_3P(O)N_4$. It can be assumed that $N_3P(O)N_4$ can easily eliminate the N_4 substituent, yielding

dx.doi.org/10.1021/ja2091867 | J. Am. Chem.Soc. 2011, 133, 20696−20699

Scheme 1. Photo-decomposition of $OP(N_3)_3$ in an Ar Matrix (N_2 Molecules Expelled from the Azides Are Omitted for Clarity)

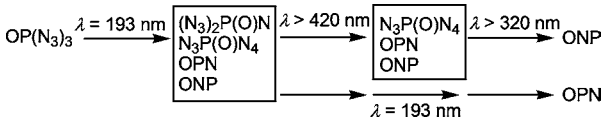

$P(O)N_3$ and 2 N_2. A similar decomposition pathway has recently been reported for the analogue $C(O)N_4$, which experienced concerted fragmentation into CO and $2N_2$.[21] $P(O)N_3$ has not been observed experimentally, since the presence of a phosphorus lone pair is expected to facilitate N_2 elimination to form OPN.

Photo-induced interconversion between OPN and ONP is of particular interest, since photochemistry obviates the large barrier predicted for thermal rearrangement of these isomers (SI Figure S7). Although this rearrangement is expected to proceed via a rather stable three-membered ONP ring, this intermediate has not been detected in photolysis experiments.

In fact, thermal decomposition of $OP(N_3)_3$ might provide an alternative route to the elusive OPN in the gas phase. Preliminary pyrolysis experiments, in which $OP(N_3)_3$ was highly diluted in Ar and directed through an electrically heated Al_2O_3 tube prior to deposition of the heated mixture as a matrix, indeed revealed the presence of OPN among the pyrolysis products. However, additional as-yet unidentified secondary products appeared, probably because of reactions of the phosphoryl intermediates with the Al_2O_3 surface. Further work is currently underway to improve the gas-phase synthesis of OPN.

■ ASSOCIATED CONTENT

Ⓢ Supporting Information

Experimental details and calculated PES of ONP isomers, calculated structures and frequencies of $(N_3)_2P(O)N$ and $N_3P(O)N_4$, experimental matrix IR difference spectra, absolute energies (in hartrees), and atomic coordinates for all optimized structures. This material is available free of charge via the Internet at http://pubs.acs.org.

■ AUTHOR INFORMATION

Corresponding Author

beckers@uni-wuppertal.de

■ ACKNOWLEDGMENTS

This work was supported by the Deutsche Forschungsgemeinschaft and the Fonds der Chemischen Industrie.

■ REFERENCES

(1) Appel, R. In *Multiple Bonds and Low Coordination in Phosphorus Chemistry*; Regitz, M., Scherer, O. J., Eds.; Thieme: Stuttgart, 1990; pp 157−219.
(2) Nixon, J. F. *Chem. Rev.* **1988**, *88*, 1327 and references therein.
(3) Gier, T. E. *J. Am. Chem. Soc.* **1961**, *83*, 1769.
(4) See for examples: (a) Kinjo, R.; Donnadieu, B.; Bertrand, G. *Angew. Chem., Int. Ed.* **2010**, *49*, 5930. (b) Weber, L. *Angew. Chem., Int. Ed.* **2010**, *49*, 5829. (c) Atkins, R.; Timms, P. L. *Spectrochim. Acta* **1977**, *33A*, 853.
(5) (a) Dulley, W. W.; Williams, D. A. A. *Interstellar Chemistry*; Academic Press: New York, 1984. (b) Yung, Y. L.; DeMore, W. B. *Photochemistry of Planetary Atmospheres*; Oxford University Press: Oxford, 1998.
(6) (a) Andrews, L.; Withnall, R. *J. Am. Chem. Soc.* **1988**, *110*, 5605. (b) Bauschlicher, C. W. Jr.; Zhou., M.; Andrews, L. *J. Phys. Chem. A* **2000**, *104*, 3566. (c) Bell, I. S.; Qian, H.-B.; Hamilton, P. A.; Davies, P. B. *J. Chem. Phys.* **1997**, *107*, 8311.
(7) Mielke, Z.; Brabson, G. D.; Andrews, L. *J. Phys. Chem.* **1991**, *95*, 75.
(8) Ahlrichs, R.; Schunck, S.; Schnöckel, H. *Angew. Chem., Int. Ed.* **1988**, *27*, 421.
(9) Bell, I. S.; Hamilton, P. A.; Davies, P. B. *Mol. Phys.* **1998**, *94*, 685.
(10) Okabayashi, T.; Yamazaki, E.; Tanimoto, M. *J. Chem. Phys.* **1999**, *111*, 3012.
(11) Busch, T.; Schoeller, W. W. *Z. Phys. D: At., Mol. Clusters* **1989**, *13*, 289.
(12) Davy, R. D.; Schaefer, H. F. III *J. Chem. Phys.* **1990**, *92*, 5417.
(13) Grant, D. J.; Dixon, D. A.; Kemeny, A. E.; Francisco, J. S. *J. Chem. Phys.* **2008**, *128*, 164305.
(14) Ziurys, L. M. *Proc. Natl. Acad. Sci. U.S.A.* **2006**, *103*, 12274.
(15) Ziurys, L. M.; Milam, S. N.; Apponi, A. J.; Woolf, N. J. *Nature* **2007**, *447*, 1094.
(16) Zeng, X. Q.; Bernhardt, E.; Beckers, H.; Willner, H. *Inorg. Chem.* **2011**, *50*, 11235.
(17) Zeng, X. Q.; Beckers, H.; Willner, H. *Angew. Chem., Int. Ed.* **2009**, *48*, 4828.
(18) Zeng, X. Q.; Beckers, H.; Willner, H.; Stanton, J. F. *Angew. Chem., Int. Ed.* **2011**, *50*, 1720.
(19) For the synthesis of ^{15}N-trisubstituted $OP(N_3)_3$, 1-^{15}N sodium azide (98 atom % ^{15}N, EURISO-TOP GmbH) was used, which in principle leads to six different isotopomers of $OP(^{15}N\text{-}N_2)_3$, where either N^{α} or N^{γ} of each azido substituent is substituted by ^{15}N.
(20) (a) Zeng, X. Q.; Beckers, H.; Willner, H.; Neuhaus, P.; Grote, D.; Sander, W. *Chem.-Eur. J.* **2009**, *15*, 13466. (b) Zeng, X. Q.; Beckers, H.; Willner, H. *Chem.-Eur. J.* **2011**, *17*, 3977.
(21) Zeng, X. Q.; Beckers, H.; Willner, H. *Angew. Chem., Int. Ed.* **2011**, *50*, 482.
(22) For a pictorial description of the HOMO and LUMO orbitals of OPN, see ref 13.
(23) Pyykkö, P.; Riedel, S.; Patzschke, M. *Chem.-Eur. J.* **2005**, *11*, 3511.